Journal of The Electrochemical Society, **158** (8) A942-A947 (2011)
0013-4651/2011/158(8)/A942/6/$28.00 © The Electrochemical Society

Electrophoretic Fabrication and Characterizations of Manganese Oxide/Carbon Nanotube Nanocomposite Pseudocapacitors

Chung Jung Hung,[a] Jeng Han Hung,[b] Pang Lin,[a] and Tseung Yuen Tseng[b,z]

[a]*Department of Materials Science and Engineering, National Chiao Tung University, Hsinchu 300, Taiwan*
[b]*Department of Electronics Engineering and Institute of Electronics, National Chiao Tung University, Hsinchu 300, Taiwan*

This study reports the electrochemical performance and stability of MnO_x-multiwall carbon nanotubes (MWCNTs) nanocomposite/Ni pseudocapacitor electrodes fabricated by a modified electrophoretic deposition (EPD) method. The nanocomposite electrode consisting of highly dispersed manganese oxide on MWCNTs was synthesized by a redox titration method at room temperature. The electrochemical properties of the electrode were demonstrated by cyclic voltammetry. The mean specific capacitances at a constant scan rate of 100 mV/s of MnO_x-MWCNTs nanocomposites without and with heat treatment at temperatures 150, 200, and 250°C for 2 h are 378, 402, 445, and 469 F/g, respectively, which indicate an increase with increasing annealing temperature. During stability tests, the as-grown MnO_x-MWCNTs nanocomposite electrode can preserve 80% of its original capacitance after 6000 cycles of operation which can be increased to 86% after annealing at 200°C for 2 h. The EPD MnO_x/MWCNTs coaxial nanocomposite pseudocapacitors with manganese oxide ionized by H^+ ion process exhibit high specific capacitance, fast reaction rate, high stability, and have high potential for practical applications.
 [DOI: 10.1149/1.3601862]

Manuscript submitted March 7, 2011; revised manuscript received May 19, 2011. Published June 16, 2011.

In recent years, manganese oxide (MnO_2) has been widely investigated as a promising pseudocapacitive material because of its low cost, abundance, more friendly environmental nature and higher electrochemical activity than other transition metal oxides. But one major issue of MnO_2 as a pseudocapacitive material is its intrinsically low electrical conductivity, which causes its poor specific capacitance. Therefore, the MnO_x/MWCNT/Ni nanocomposite electrode was employed for pseudocapacitor applications in our previous study[1] to enhance the specific capacitances. The specific capacitances were 415 and 388 F/g at scan rates of 5 and 100 mV/s, respectively. However, the capacitance of the nanocomposite remained only at 79% of the original value after 1000 cycles. Such degradation was caused by MnO_2 nanoparticles detached from the surface of the nanocomposites.

Obviously, uniform surface distribution of the MnO_2 nanoparticles (or film) coated onto CNTs and the good adhesion between MnO_2 nanoparticles (or film) and CNTs are necessary to improve the stability of the pseudocapacitors. Up to now, only a few papers have appeared in the literature that report to improve the adhesion and uniform surface distribution of MnO_2 coated onto CNTs. The combination of vacuum infiltration and chemical vapor deposition process has been employed to form the uniform MnO_2/CNT hybrid nanostructure[2]. Besides, the application of direct redox deposition-precipitation method for the preparation of MnO_2/CNT nanocomposite powders could enhance the adhesion and electrical contact between the MnO_2 and the CNT.[3–9] Various methods reported in those papers can be utilized to fabricate the electrode for making pseudocapacitor, which include mechanical process and electrophoretic deposition (EPD). In a mechanical process, the slurry consisting of active powder and binder has been pressed on the current collector.[3,4] Creation of positive charges on the surfaces of MnO_2/CNTs nanocomposites can be achieved by absorbing some surfactants in sodium alginate,[10] polyethylene,[11] or dopamine[12] polymer solutions in their surfaces so that they can be dispersed uniformly in solvents and directly deposited on the current collector by using EPD method. However, the binders or the surfactants used in the above methods were regarded as high charge transfer resistance materials to lower efficient charge/electron transport from the current collector to the active materials.

Therefore, it is an important issue to develop a processing method to fabricate a binder-free MnO_x-CNTs nanocomposite pseudocapacitor electrode with a low contact resistance between the nanocomposite and the current collector for making high performance pseudocapacitors. Such a good interfacial adhesion between MnO_x nanoparticles (or film) and CNTs can be expected to improve the pseudocapacitance behavior of nanocomposite electrode.

In this study, the MnO_x-MWCNTs nanocomposite/$Ni_{substrate}$ electrode is prepared by a modified EPD technique using hydrogen ion instead of polymer as surfactant to ionize the surface of MnO_x. The nanocomposites are synthesized by redox titration method at room temperature. The MnO_x is uniformly coated onto the surface of CNTs. The charge transfer resistance between the MnO_x-MWCNTs nanocomposite and the current collector is significantly improved through such an EPD method. The electrochemical performances of the MnO_x-MWCNTs nanocomposite/$Ni_{substrate}$ pseudocapacitors are also reported.

Experimental

The MnO_x-MWCNTs nanocomposite thin films were directly deposited onto $10 \times 30 \times 1$ mm flat Ni substrates by electrophoretic deposition technique in this study. The Ni substrates were etched with 10% nitric acid solution for 30 min to obtain rough surface and cleaned with deionized (DI) water in an ultrasonic bath, and dried in an oven at 100°C for 12 h. The commercial MWCNTs (specific surface area: 40–300 m^2/g, length: 5–20 μm) were purified by putting them in boiling 70% nitric acid solution for 24 h, cleaned with DI water and dried in an oven at 100°C for 12 h before synthesizing MnO_x/MWCNTs nanocomposites.

The pseudocapacitor electrode material, MnO_x/MWCNTs nanocomposite powders were synthesized by redox titration method at room temperature. The purified MWCNTs were put in the 0.005 M $KMnO_4$ solution and dispersed by ultrasonic agitation for 30 min. Then 0.016 M $MnSO_4$ was added into the MWCNTs/$KMnO_4$ solution drop by drop at room temperature. Such a solution was stirred for 6 h until the disappearance of its purple color. Finally, the nanocomposites were obtained via filtering the solution and cleaned by DI water and dried in an oven at 110°C for 12 h.

Then the MnO_x/MWCNTs nanocomposite film was deposited on the Ni substrate via electrophoretic deposition (EPD). The electrolyte used in EPD was a mixture of 0.24 g MnO_x/MWCNTs nanocomposite powders and 37% hydrochloric acid (0.4 ml) in isopropyl alcohol (200 ml). The powders were dispersed well in the solution by ultrasonic agitation for 30 min. Nickel and platinum foils were put in this solution as cathode and anode at a distance of 1 cm, respectively. The MnO_x/MWCNTs nanocomposite powders were

[z] E-mail: tseng@cc.nctu.edu.tw

electrophoretically deposited on the Ni substrate after a direct current (DC) voltage of 30 V was applied for 40 min. After EPD, the nanocomposite film formed on Ni substrate was dried in an oven at 100°C for 12 h, which names as-grown nanocomposite electrode. The weight of the deposited nanocomposite film was measured by a microbalance (PRECISA XR125SM-FR) with an accuracy of 0.1 μg. The loading of nanocomposites film on Ni substrate was about 47.5 ± 5.7 μg.

In order to know the effect of annealing temperature on capacitive behavior of MnO_x/MWCNTs nanocomposite pseudocapacitors, the as-grown nanocomposite films were annealed at 150, 200, and 250°C in air atmosphere for 2 h, respectively.

A field emission scanning electron microscope (FESEM, JEOL JSM-6500) and X-ray diffractometer (XRD, Bode D1) were used to analyze surface morphology and crystallization of the film, respectively. The oxidation states of manganese oxide film were examined by X-ray photoelectron spectroscopy (XPS, ULVAC-PHI Quantera SXM). Field emission transmission electron microscope (FETEM, JEOL JEM-2100F) was used to observe the coaxial structure of MnO_x/MWCNTs nanocomposite material. The specific surface area of the nanocomposite material was determined by BET (Brunauer, Emmett and Teller method) surface area analyzer. Thermal analysis was performed from 50 to 800°C at 4°C/min ramping rate under air atmosphere using thermogravimetric analyzer (TGA, TA Instruments Q500).

The electrochemical performance of the pseudocapacitors were measured by cyclic voltammetry (CV), galvanostatic charge/discharge cycling (CC) and electrochemical impedance spectroscopy (EIS) using CH Instruments 618B electrochemical analyzer. Electrochemical measurements were carried out in a three-electrode cell with a saturated calomel reference electrode (SCE), a counter electrode of platinum sheet, and aqueous 0.1 M Na_2SO_4 as the electrolyte. CVs were recorded between 0 and 0.8 V versus SCE at a scan rate varied from 5 to 100 mV/s. The CC testing was recorded between 0 and 0.8 V versus SCE at a constant current 1 mA. The values of the specific capacitance (F/g) were estimated from cyclic voltammetric curve by using the following equation

$$C = \frac{Q}{\Delta E \times m}$$

where m is the mass of the active material, Q the voltammetric charge within the working voltage, and ΔE the width of the potential window.

Impedance spectroscopy investigation was performed in the frequency range of 1 mHz ~100 kHz at a voltage of 100 mV with an AC amplitude of 5 mV.

Results and Discussion

The FESEM surface morphology of as-grown nanocomposite film is shown in Fig. 1a, indicating that a highly porous MnO_x-MWCNTs nanocomposite layer electrophoretically deposited on the Ni substrate. It shows that the MnO_x is homogenously uniformly coated on the MWCNTs surface by redox titration method.

The average specific surface area of MnO_x-MWCNTs nanocomposites from BET measurement is 170.88 m^2/g. This surface area is much larger than that (59–131 m^2/g) reported in our previous study,[1] in which the MnO_x nanoparticles were deposited on MWCNTs by using EPD. Such a porous MnO_x-MWCNTs nanocomposite film would provide a large redox reaction area. The density and the thickness of the nanocomposite film are about 0.41 g/cm^3 and 1167 nm, respectively. The average thickness of MnO_x layer in the nanocomposite film is about 4 nm according to the TEM image shown in Fig. 1b.

The TGA and DSC curves were used to detect the thermal stability of the as-grown MnO_x-MWCNTs nanocomposites. From the TGA curve of Fig. 2, the weight loss below 250°C is attributed to evaporation of physically adsorbed water. The DSC curve depicts

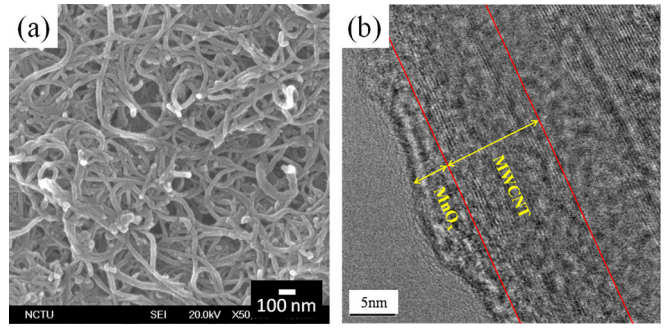

Figure 1. (Color online) SEM image (a) and TEM image (b) of as-grown MnO_x-MWCNTs nanocomposite electrode.

that the removal of volatile ingredient and water from the as-grown nanocomposites results in about 68% weight loss.

Figure 3 shows the XRD patterns of the as-grown and annealed MnO_x-MWCNTs nanocomposite/$Ni_{substrate}$ electrodes. The annealing temperatures are 150, 200 and 250°C. Excluding peaks at 44.5, 51.9, and 76.5° corresponding to the diffraction peaks of pristine Ni substrate, no other Bragg peaks appear. It demonstrates that the MnO_x-MWCNTs nanocomposites without and with annealing process exhibit amorphous structure. It has been shown in the previous paper that the better electrochemical performance was obtained for the pseudocapacitor with oxide electrode containing higher amount of amorphous structure.[13] Such amorphous structure could cause the electrolyte inserting into the matrix easily, leading to an increase in the reaction area between electrolyte and active electrode materials.[14] The amorphous structure of manganese oxide, (Fig. 3) used in the pseudocapacitors as an electrode is expected to have a rapid oxidation-reduction reaction rate.

In this work cyclic voltammetry measurement (CV) was employed to understand the capacitive behavior of the pseudocapacitor materials. Figure 4 shows the CV curves of the MnO_x-MWCNT nanocomposite/$Ni_{substrate}$ electrode in neutral aqueous electrolyte (0.1 M Na_2SO_4) at 25°C in the potential in the range $0 < E_{SCE} < 0.8$ V versus SCE with scan rates of 5, 25, 50, 75 and 100 mV/s. The typical CV curves of the nanocomposite electrode are almost a near-ideal rectangular and symmetric profile and no redox peaks appear in the cycling potential from 0 to 0.8 V. It has been well established that the nanocomposite electrode exhibits excellent capacitive behavior.

The variation of measured specific capacitances with scan rate is indicated in the inset of Fig. 4. It is shown that the mean specific capacitances of the electrode with scan rates of 5, 25, 50, 75, and 100 mV/s are 480, 432, 411, 393, and 378 F/g, respectively. The

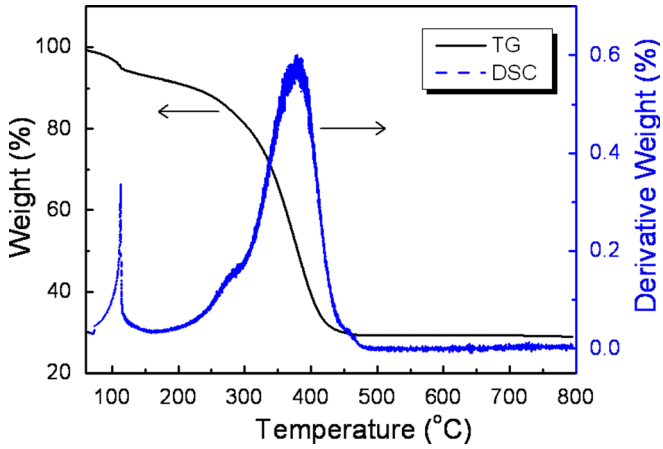

Figure 2. (Color online) TGA curve of MnO_x-MWCNTs nanocomposites synthesized by redox titration method.

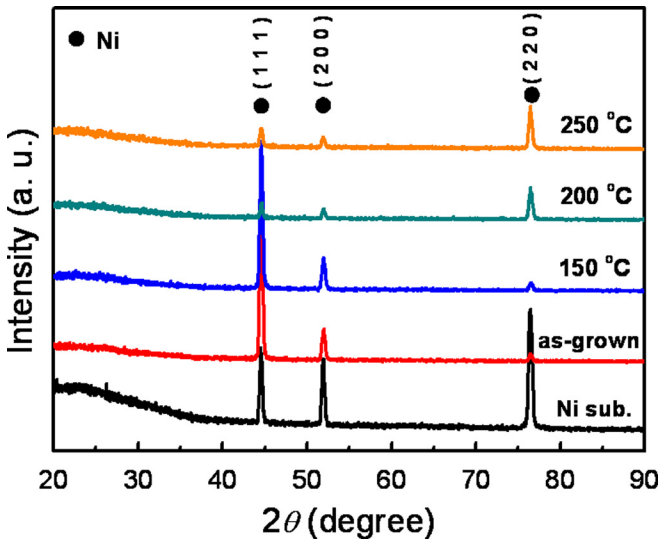

Figure 3. (Color online) XRD patterns of the as-grown and annealed MnO_x/MWCNTs nanocomposite electrodes with heat treatment temperature 150, 200, and 250°C.

specific capacitance at the potential scan rate of 100 mV/s of the nanocomposite electrode is 78.8% of that measured with a scan rate of 5 mV/s.

Figure 5 depicts the CV curves of the MnO_x-MWCNTs nanocomposite electrodes annealed at different temperatures with a constant scan rate of 100 mV/s. The typical CV curves are a nearly rectangular profile and some redox peaks in the curves appear as the annealing temperature increase. The CV loop area increases with an increase in the annealing temperature due to the enhancement of the capacitance. The mean specific capacitances of the as-grown and 150, 200, and 250°C annealed nanocomposite electrodes are 378, 402, 445, and 469 F/g, respectively, at a constant scan rate 100 mV/s. The specific capacitance increases around 25% as shown in the inset of Fig. 5 after the nanocomposite is annealed at 250°C.

For the purpose of observation on the connection between oxidation state of Mn in manganese oxide film and charge storage mechanism, the nanocomposite electrodes annealed at different temperatures were analyzed by XPS. Figure 6 indicates the $Mn2p^{3/2}$ spectra of the as-grown and 150, 200 and 250°C annealed electrodes. The curve fitting of the obtained XPS curve demonstrates that the manganese oxide film is composed of Mn_3O_4 and MnO_2. It has been reported that the binding energies of Mn-O of the $Mn2p^{3/2}$ orbit for Mn^{3+} and Mn^{4+} are 641.6 and 642.6 eV, respectively.[15–18]

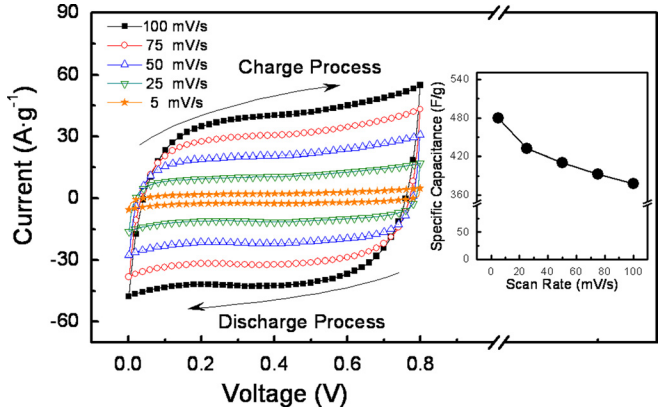

Figure 4. (Color online) CV curve of as-grown MnO_x-MWCNTs nanocomposite electrode in 0.1 M Na_2SO_4 at scan rates of 5, 25, 50, 75 and 100 mV/s. (The inset is the specific capacitance at various scan rates).

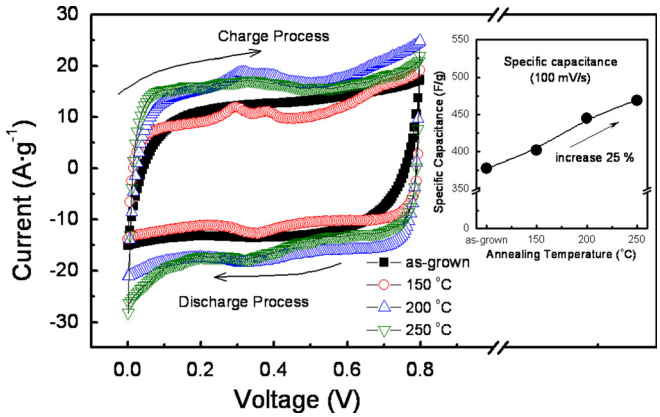

Figure 5. (Color online) CV curve of the as-grown and annealed MnO_x/MWCNTs nanocomposite electrodes in 0.1 M Na_2SO_4 at a constant scan rate of 100 mV/s with various annealing temperatures of 150, 200, and 250°C. (The inset shows the specific capacitance at various annealing temperatures).

According to the areas of XPS peaks, the ratio of MnO_2/Mn_3O_4 for as-grown nanocomposite can be estimated to be 1.88. With increasing annealing temperature up to 200°C, the MnO_2/Mn_3O_4 ratio rapidly increases to 4.29. The correlation among the specific capacitance, MnO_2/Mn_3O_4 ratio and charge storage mechanism is explained as follows. Two chemical reactions at 25°C are proposed to explain the MnO_2 or Mn_3O_4 charge storage behavior

$$MnO_2 + H_2O + e^- = MnO \cdot OH + OH^- \quad \Delta G = -5.305 \text{ kcal} \cdot \text{mol}^{-1} \quad [1]$$

$$Mn_3O_4 + 2H_2O = 3MnO \cdot OH + H^+ + e^- \quad \Delta G = 13.370 \text{ kcal} \cdot \text{mol}^{-1} \quad [2]$$

The charge/discharge mechanism of manganese oxide has been also proposed in literature[19]

$$MnO_x(OH)_y + \delta H^+ + \delta e^- \leftrightarrow Mn_{x-\delta}(OH)_{y+\delta} \quad [3]$$

where $MnO_x(OH)_y$ and $MnO_{x-\delta}(OH)_{y+\delta}$ indicate the higher and lower oxidation state of Mn, separately. Based on above equations, the manganese oxide is transformed into the hydrated manganese oxide, MnO·OH before charge/discharge process. From thermodynamic point of view, it is a spontaneous process from MnO_2 to MnO·OH according to reaction 1, due to a negative Gibbs free energy change while the Mn_3O_4 to MnO·OH process is a non-spontaneous reaction according to reaction 2, where Gibbs free energy change is a positive value. Therefore, the specific capacitance of the MnO_x-MWCNT nanocomposite/$Ni_{substrate}$ electrode is increased with an increase in annealing temperature which is due to the higher MnO_2 content in the nanocomposite electrode heat treated at higher temperature.

The effect of annealing temperature on the electrochemical characteristics can be demonstrated from electrochemical impedance spectrum and the corresponding equivalent circuit model. The Nyquist plots of the AC impedance responses for the nanocomposite electrodes annealed at various temperatures in 0.1 M Na_2SO_4 electrolyte are shown in Fig. 7, indicating that all spectra contain a semicircle (inset of Fig. 7) in the high frequency region (>25.7 Hz), a straight line inclined at a constant phase in the mid-frequency region (3.7 ~ 25.7 Hz), and an almost vertical capacitive line in the low frequency region (<3.7 Hz). Such a pattern of the impedance spectra can be fitted by an equivalent circuit shown in the inset of Fig. 7. Here, R_b represents the bulk resistance of the electrochemical system, which is used to account for electrical conductivity of the electrolyte and electrodes; R_{ct} and C_{dl} are the charge-transfer resistance on the surface of the electrode in contact with the electrolyte and its

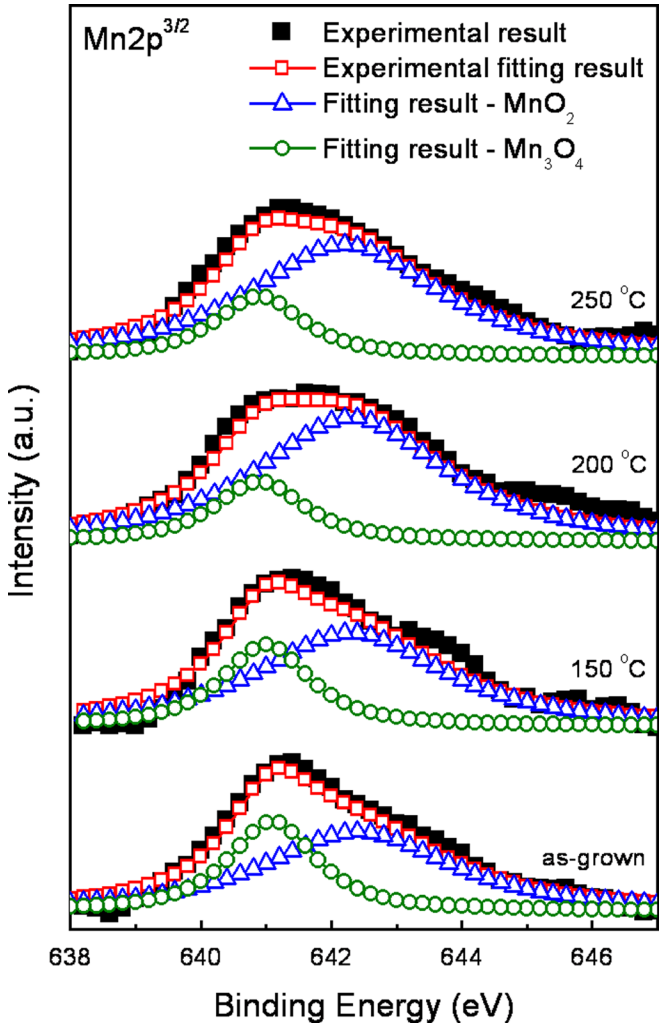

Figure 6. (Color online) $Mn2p^{3/2}$ spectra of the as-grown and annealed MnO_x/MWCNTs nanocomposite electrodes with annealing temperatures indicated.

relative double layer capacitance, respectively, corresponding to the semicircle at high frequencies; W is the Warburg impendence related to a combination of the ionic diffusion at the interface between the active electrode material and electrolyte[20–22] which is employed to fit the straight line at intermediate frequencies (Fig. 7). Followed by a near-vertical line at low frequency region (close to 0.001 Hz), it is a typical capacitive behavior.

A vertical straight line in the imaginary positive part (-Im(Z)>0) of the Nyquist plot basically corresponds to an ideal capacitance element. In fact, the MnO_x-MWCNTs nanocomposite electrode regards as a pseudocapacitor with capacitance originating from faradic reaction rather than an electrical double layer capacitor (EDLC). Therefore, the semicircle appearing at high frequencies should be related to above electrochemical reaction 3 used for to explaining the charge/discharge mechanism of MnO_2. Additionally, based on the inset of Fig. 7, it can be seen that the radius of the semicircle is declined when annealing temperature increased. It means that the reduction of charge transfer resistance R_{ct} that is considered as a barrier of Na^+ insertion/extraction lead to more MnO_x available to charge and discharge during cycling. From impedance analysis the increase in specific capacitance after thermal treatment can be referred to enlargement of suitable redox sites for Na^+ ions.

From Bode plot (log|Z| *vs.* log f) shown in Fig. 8a, the high frequency region yields slopes of close to zero (∼−0.018 & −0.16), which are the characteristic of a pure resistor. At the low frequency

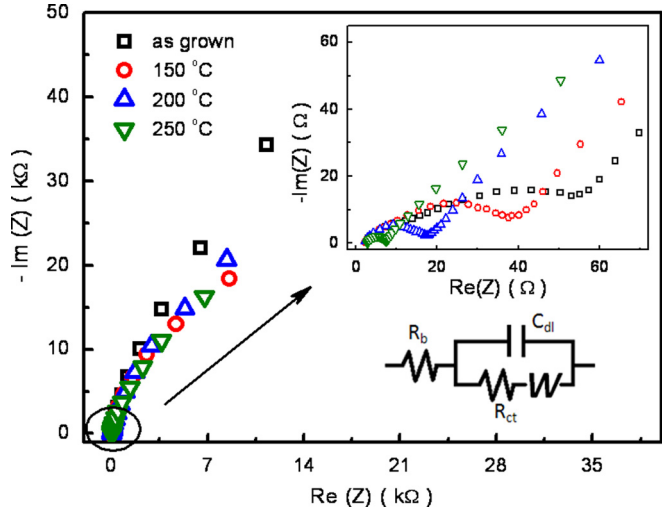

Figure 7. (Color online) Impedance analysis of the as-grown and annealed MnO_x/MWCNTs nanocomposite electrodes with annealing temperatures indicated. The insets show the enlargement portion of selected part indicated and equivalent circuit of the pseudocapacitor, respectively.

region, if yielding a slope of <1.0, it indicates the characteristic of a pseudocapacitor. These results suggest that the behavior of the nanocomposite electrode changes from a pure resistor at high frequency to a pseudocapacitors at low frequency. In addition, on the basis of the other type of Bode plot (-phase angle (degree) vs. log f) shown in Fig. 8b, the phase angle is closed to 80°, which deviates from an ideal capacitive behavior (phase angle = 90°).[23] This nonideal behavior is believed due to the presence of pseudocapacitive nature of the MnO_x-MWCNTs nanocomposite.

We have developed a novel method of ionizing the surface of MnO_x with hydrogen ion as surfactant to substitute polymer by electrophoretic deposition method. Furthermore, the preparation of nanocomposite pseudocapacitor electrode with the binder-free or the surfactants-free was regarded as the method to decrease the charge transfer resistance and to increase efficient charge/electron transport from the current collector to the active materials.

In our experiment, the long-term stability test of the MnO_x-MWCNTs nanocomposite electrode for pseudocapacitors was a

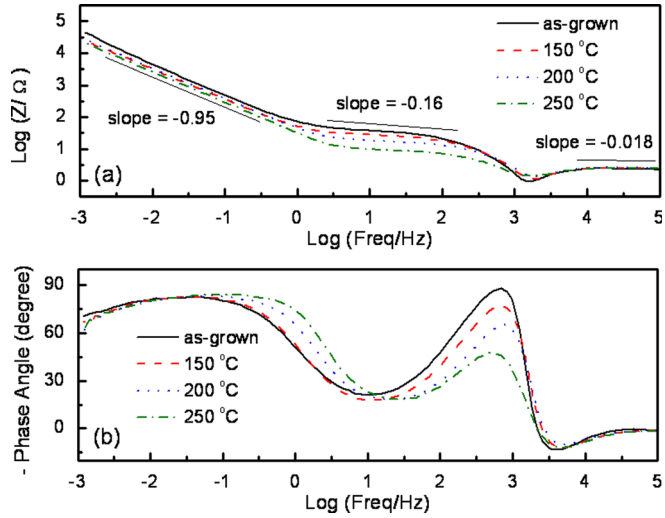

Figure 8. (Color online) Typical Bode plots for the MnO_x-MWCNTs nanocomposite electrode (a) log|Z| *vs.* log f, (b) -phase angle (degree) vs. log f.

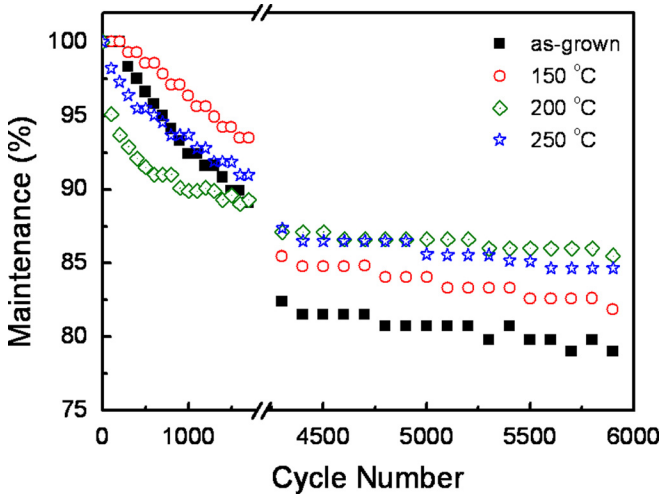

Figure 9. (Color online) Stability test of the as-grown and annealed MnO_x/MWCNTs composite electrodes with annealing temperatures indicated via a constant current 1 mA charge/discharge process.

charge/discharge test with 1 mA constant current. The dependence of the maintenance efficiency on specific capacitances for the as-grown and annealed nanocomposite electrodes is shown in Fig. 9. It is indicated that the specific capacitances of the as-grown and annealed nanocomposite electrodes all slightly decrease to 93% of the initial values after about 1000 cycles. Finally, it displays that they all can maintain above 80% after long cycling and the maintenance efficiency of the capacitance increases with increasing annealing temperature up to 200°C and the highest efficiency can reach about 86% after 6000 cycles for both 200 and 250°C annealed electrodes. The above results are attributed to the enhancement of the amount of MnO_2 species after annealing and good adhesion between manganese oxide and MWCNTs of the nanocomposite electrode, leading to reduced dissolution of MnO_2 film during the charge/discharge process.

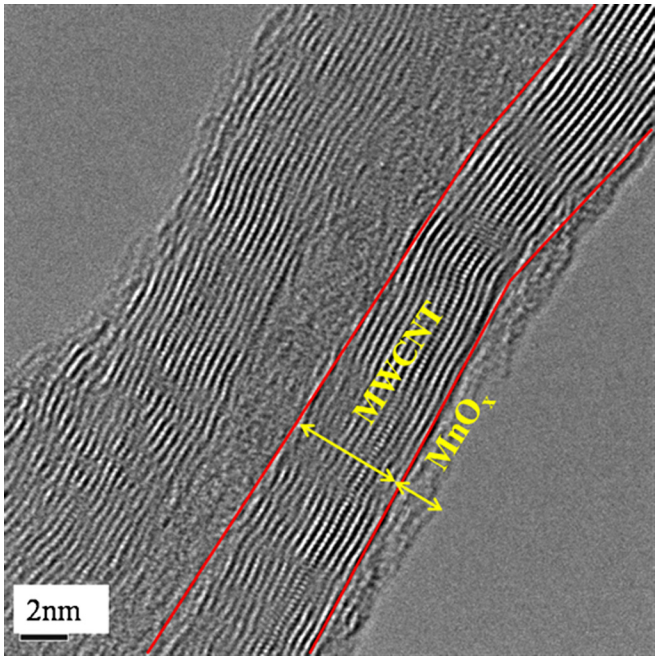

Figure 10. (Color online) TEM image of as-grown MnO_x-MWCNTs nanocomposite electrode after 6000 cycles test.

TEM observation is carried out to understand the influence of long cycling on the morphology of the as-grown nanocomposite electrode. The TEM image of the nanocomposite after galvanostatic charge/discharge 6000 cycles is shown in Fig. 10. The thickness of manganese oxide decreases from 4 nm before cycling (Fig. 1b) to around 2 nm after cycling. When measuring from 0.8 to 0 V during cycling, the MnO_x film is reduced and some is dissolved into the electrolyte as Mn^{2+} cations.[15] During scanning from 0 to 0.8 V, some of the dissolved Mn^{2+} cations transform into MnO_x and deposit on the electrode's surface again. Comparing to our previous study[1] in which the capacitance of the nanocomposite kept only at 79% after 1000 cycles due to some MnO_x nanoparticles detached from the nanocomposite, this study shows much better stability result. This low degradation of specific capacitance is attributed to better adhesion between MnO_x and MWCNTs, which can reduce the dissolution of MnO_x film and remain the surface morphology after 6000 cycling test.

Conclusions

In summary, we have developed a novel method of ionizing the surface of manganese oxide with hydrogen ion instead of polymer material surfactant to fabricate pseudocapacitor electrode by EPD. The nanocomposites composed of high dispersion of MnO_x on the surface of MWCNTs were synthesized by redox titration method at room temperature. With the help of such nanocomposite electrode, the degradable capacitance caused by dissolution and detachment of MnO_x during the charge/discharge process can be significantly improved. The as-grown MnO_x-MWCNTs nanocomposite electrode can keep about 80% of its original capacitance after 6000 charge/discharge cycles.

The amorphous structured nanocomposite electrode annealed at 250°C allows Na^+ ion to fast insert and extract. The XPS analysis result indicates that the MnO_x film is composed of MnO_2 and Mn_3O_4. The amount of MnO_2 species in the nanocomposites increased with an increase of annealing temperature. The mean specific capacitance at 100 mV/s of as-grown nanocomposite, 378 F/g can increase to 469 F/g for the nanocomposite after annealing at 250°C for 2 h. This enhancement is attributed to the MnO_2/Mn_3O_4 ratio changed from 1.88 (as-grown) to 4.29 (250°C annealed). The charge transfer resistance (a barrier for Na^+ insertion and extraction) decreases with such an increase of MnO_2 on the basis of impedance analysis. The 200°C annealed MnO_x-MWCNTs nanocomposite electrode can maintain about 86% of its original capacitance after 6000 charge/discharge cycles. Our EPD MnO_x/MWCNTs coaxial nanocomposite pseudocapacitors exhibiting the high specific capacitance, fast reaction rate, and high stability, have high potential for practical applications.

Acknowledgment

This work was supported by the National Science Council of ROC under contract no. NSC 99-2221-E-009-064-MY3.

References

1. C. Y. Lee, H. M. Tsai, H. J. Chuang, S. Y. Li, P. Lin, and T. Y. Tseng, *J. Electrochem. Soc.*, **152**, A716 (2005).
2. A. L. M. Reddy, M. M. Shaijumon, S. R. Gowda, and P. M. Ajayan, *Nano Lett.*, **9**, 1002 (2009).
3. J. Yan, Z. Fan, T. Wei, J. Cheng, B. Shao, K. Wang, L. Song, and M. Zhang, *J. Power Sources*, **194**, 1202 (2009).
4. E. R. Piñero, V. Khomenko, E. Frackowiak, and F. Béguin, *J. Electrochem. Soc.*, **152**, A229 (2005).
5. T. Bordjiba and D. Bélanger, *J. Electrochem. Soc.*, **156**, A378 (2009).
6. Y. Wang, H. Liu, X. Sun, and I. Zhitomirsky, *Scr. Mater.*, **61**, 1079 (2009).
7. X. Jin, W. Zhou, S. Zhang, and G. Z. Chen, *Small*, **3**, 1513 (2007).
8. S. B. Ma, K. W. Nam, W. S. Yoon, X. Q. Yang, K. Y. Ahn, K. H. Oh, and K. B. Kim, *J. Power Sources*, **178**, 483 (2008).
9. V. Subramanian, H. Zhu, and B. Wei, *Electrochem. Commun.*, **8**, 827 (2006).
10. J. Li and I. Zhitomirsky, *J. Mater. Process. Technol.*, **209**, 3452 (2009).
11. J. Li and I. Zhitomirsky, *Colloids Surf., A*, **348**, 248 (2009).
12. Y. H. Wang and I. Zhitomirsky, *Langmuir*, **25**, 9684 (2009).
13. H. Y. Chu, Q. Y. Lai, L. Wang, J. F. Lu, and Y. Zhao, *Ionics*, **16**, 233 (2010).
14. C. C. Hu and T. W. Tsou, *J. Power Sources*, **115**, 179 (2003).

15. C. H. Liang and C. S. Hwang, *Jpn. J. Appl. Phys.*, **47**, 1662 (2008).
16. S. Chou, F. Cheng, and J. Chen, *J. Power Sources*, **162**, 727 (2006).
17. M. Chigane, M. Ishikawa, and M. Izaki, *J. Electrochem. Soc.*, **148**, D96 (2001).
18. M. Toupin, T. Brousse, and D. Be'langer, *Chem. Mater.*, **16**, 3184 (2004).
19. A. R. Boccaccini, J. Cho, J. A. Roether, B. J. C. Thomas, E. J. Minay, and M. S. P. Shaffer, *Carbon*, **44**, 3149 (2006).
20. W. Wei, X. Cui, W. Chen, and D. G. Ivey, *J. Power Sources*, **186**, 543 (2009).
21. M. W. Xu, D. D. Zhao, S. J. Bao, and H. L. Li, *J. Solid State Electrochem.*, **11**, 1101 (2007).
22. S. S. Zhang, K. Xu, and T. R. Jow, *Electrochim. Acta*, **49**, 1057 (2004).
23. A. T. Chidembo, K. I. Ozoemena, B. O. Agboola, V. Gupta, G. G. Wildgoose, and R. G. Compton, *Energy Environ. Sci.*, **3**, 228 (2010).